DR. STEFANIE L VOGT (Orcid ID : 0000-0002-0393-5712)

Article type : Research Article

Characterization of the *Citrobacter rodentium* Cpx regulon and its role in host infection

Stefanie L. Vogt[a], Roland Scholz[a], Yun Peng[b], Randi L. Guest*[b], Nichollas E. Scott*[a], Sarah E. Woodward[a,c], Leonard J. Foster[a,d], Tracy L. Raivio[b]#, and B. Brett Finlay[a,c,d]#

[a]Michael Smith Laboratories, University of British Columbia, Vancouver, BC, Canada
[b]Department of Biological Sciences, University of Alberta, Edmonton, AB, Canada
[c]Department of Microbiology and Immunology, University of British Columbia, Vancouver, BC, Canada
[d]Department of Biochemistry and Molecular Biology, University of British Columbia, Vancouver, BC, Canada

#Address correspondence to B. Brett Finlay, bfinlay@interchange.ubc.ca, +1 (604) 822-2210, or Tracy L. Raivio, traivio@ualberta.ca, +1 (780) 492-3491.

*Present address:
Randi L. Guest: Department of Molecular Biology, Lewis Thomas Lab, Princeton University, Princeton, NJ 08544
Nichollas E. Scott: Department of Microbiology and Immunology, University of Melbourne at the Peter Doherty Institute for Infection and Immunity, Parkville, Victoria 3010, Australia

This is the author manuscript accepted for publication and has undergone full peer review but has not been through the copyediting, typesetting, pagination and proofreading process, which may lead to differences between this version and the Version of Record. Please cite this article as doi: 10.1111/mmi.14182

Running Title: Role of Cpx Regulon in *C. rodentium* Infection

Keywords: *Citrobacter rodentium*, Bacterial Gene Expression Regulation, Periplasmic Proteins, Virulence, Disulfides

Summary

Envelope-localized proteins, such as adhesins and secretion systems, play critical roles in host infection by Gram-negative pathogens. As such, their folding is monitored by envelope stress response systems. Previous studies demonstrated that the Cpx envelope stress response is required for virulence of *Citrobacter rodentium*, a murine pathogen used to model infections by the human pathogens enteropathogenic and enterohemorrhagic *Escherichia coli*; however, the mechanisms by which the Cpx response promotes host infection were previously unknown. Here, we characterized the *C. rodentium* Cpx regulon in order to identify genes required for host infection. Using transcriptomic and proteomic approaches, we found that the Cpx response upregulates envelope-localized protein folding and degrading factors but downregulates pilus genes and type III secretion effectors. Mouse infections with *C. rodentium* strains lacking individual Cpx-regulated genes showed that the chaperone/protease DegP and the disulfide bond oxidoreductase DsbA were essential for infection, but Cpx regulation of these genes did not fully account for attenuation of *C. rodentium ΔcpxRA*. Both deletion of *dsbA* and treatment with the reducing agent dithiothreitol activated the *C. rodentium* Cpx response, suggesting that it may sense disruption of disulfide bonding. Our results highlight the importance of envelope protein folding in host infection by Gram-negative pathogens.

Introduction

The Gram-negative envelope, which consists of the inner and outer membranes (IM and OM) and intervening periplasmic space, plays a critical role in the cell's interactions with its environment. Envelope-localized proteins perform essential functions including nutrient uptake, extrusion of waste and toxic molecules, electron transport, adherence to surfaces, motility, and signal transduction, among others. As such, bacteria require a means for sensing and correcting problems with protein folding in the envelope. Among the numerous envelope stress responses present in enterobacteria, the Cpx envelope stress response plays a particularly important role in monitoring the folding of periplasmic and IM proteins (Vogt and Raivio, 2012; Raivio, 2014;

Guest and Raivio, 2016). The Cpx response is mediated by a two-component system consisting of the IM-localized histidine kinase CpxA and the cytoplasmic response regulator CpxR. Several activating cues for *Escherichia coli* CpxA have been identified, including alkaline pH, alterations to the phospholipid composition of the IM, and expression of exogenous pilin proteins in the absence of their cognate chaperones (Jones *et al.*, 1997; Mileykovskaya and Dowhan, 1997; Danese and Silhavy, 1998; Nevesinjac and Raivio, 2005). Although the molecular nature of the CpxA activating cue is still unknown, all of the known inducing conditions are expected to generate misfolded proteins in the envelope. Activation of CpxA causes it to autophosphorylate at a conserved histidine residue and subsequently act as a CpxR kinase (Raivio and Silhavy, 1997). Phosphorylated CpxR then acts as a transcription factor to activate or repress transcription of dozens of genes. In *E. coli*, in which the Cpx regulon has been best characterized, CpxR activates expression of a suite of periplasmic chaperones and proteases (such as *degP*, *dsbA*, *ppiA*, and *spy*) and represses expression of envelope-localized protein complexes such as flagella (Danese *et al.*, 1995; Danese and Silhavy, 1997; Pogliano *et al.*, 1997; De Wulf *et al.*, 1999; Raivio *et al.*, 2000; De Wulf *et al.*, 2002; Raivio *et al.*, 2013). By increasing the cell's capacity to degrade or refold envelope proteins while also reducing the flux of proteins entering the envelope, the Cpx response reduces the burden of misfolded proteins in the envelope compartment.

Given the many envelope-localized proteins that play a crucial role in pathogens' ability to infect their hosts, such as fimbrial and non-fimbrial adhesins and secretion systems, it is unsurprising that envelope stress responses are essential for the virulence of many pathogens (Raivio, 2005; Vogt and Raivio, 2012). The effect of the Cpx response on expression of virulence determinants has been particularly well studied in attaching and effacing (A/E) pathogens. A/E organisms are a group of non-invasive diarrheal pathogens including the human pathogens enteropathogenic *E. coli* (EPEC) and enterohemorrhagic *E. coli* (EHEC) (Moon *et al.*, 1983; Sherman *et al.*, 1988; reviewed in Croxen *et al.*, 2013). A/E pathogens initially adhere to the host intestinal epithelium using pili – typical EPEC strains use the bundle-forming pilus (BFP) for this purpose (Girón *et al.*, 1991; Cleary *et al.*, 2004). Subsequently, the pathogen uses a type III secretion system (T3SS) encoded by the locus of enterocyte effacement (LEE) pathogenicity island to inject a number of effector proteins into the host cytoplasm.

The Cpx response is known to affect expression of both pili and T3SSs that are essential for A/E pathogen virulence. Studies in EPEC and EHEC have examined the effect of two opposing changes to Cpx activity: the Cpx response can be inactivated through mutation of *cpxR*, or it can be constitutively activated – for example, by introducing signal-blind mutations into CpxA that cause it to constitutively phosphorylate CpxR. When the Cpx response is inactivated in EPEC, abundance of the BFP proteins is reduced, as is EPEC's ability to adhere to cultured human cells (Nevesinjac and Raivio, 2005). Decreased pilus elaboration in the absence of Cpx pathway activity has been attributed to reduced expression of envelope-localized protein folding factors, including DsbA, DegP, and CpxP, which have been shown to promote stability of pilus component proteins (Zhang and Donnenberg, 1996; Vogt *et al.*, 2010; Humphries *et al.*, 2010). However, inactivation of *cpxR* has little effect on the transcription of the *bfp* genes or the expression and *in vitro* functionality of the T3SS in EPEC and EHEC (MacRitchie *et al.*, 2008; De la Cruz *et al.*, 2016). Conversely, constitutive Cpx activation dramatically reduces expression of the BFP in EPEC and the T3SS in both EPEC and EHEC (MacRitchie *et al.*, 2008; Vogt *et al.*, 2010; De la Cruz *et al.*, 2016). Repression of the BFP when the Cpx response is activated occurs primarily at the level of transcription of the *bfp* genes, while repression of the T3SS involves both transcriptional and post-translational effects (MacRitchie *et al.*, 2008; Vogt *et al.*, 2010; MacRitchie *et al.*, 2012). Together, these results suggest that, at basal levels of pathway activity, the Cpx response promotes biogenesis of pili by enhancing expression of envelope protein chaperones and proteases; however, when the Cpx pathway is strongly activated, expression of pili and the T3SS is repressed, which may help to reduce protein traffic to the envelope. These studies provided a great deal of insight into the molecular mechanisms by which the Cpx response regulates expression of EPEC and EHEC virulence factors; however, they could not answer the question of whether the Cpx response would be beneficial to these A/E pathogens *in vivo*.

Both EPEC and EHEC are human-specific pathogens that have a limited ability to colonize the mouse intestine and do not produce symptoms of disease in mice that reflect those observed in human infections (Mundy *et al.*, 2006). For this reason, *Citrobacter rodentium*, a natural pathogen of mice that also carries the LEE, is frequently used to model A/E infections (Collins *et al.*, 2014). In many strains of mice, including C57BL/6, *C. rodentium* infection leads to self-limiting colitis that resolves approximately three weeks post-infection (Simmons *et al.*,

2002). However, in susceptible strains such as C3H/HeJ, infection with wild-type *C. rodentium* is lethal within six to ten days (Vallance *et al.*, 2003).

The effect of a *ΔcpxRA* loss-of-function mutation on the ability of *C. rodentium* to infect its host was previously examined (Thomassin *et al.*, 2015; Thomassin *et al.*, 2017). The *ΔcpxRA* mutant is severely attenuated in its ability to infect both C57BL/6 and C3H/HeJ mice. Compared to wild-type *C. rodentium*, the *ΔcpxRA* mutant produces fewer histopathological changes in C57BL/6 mice and causes no mortality in C3H/HeJ mice; both of these changes may be related to the significantly lower level of gut colonization by the *ΔcpxRA* mutant (Thomassin *et al.*, 2015). However, since the *ΔcpxRA* mutant has no defect in growth or T3S *in vitro* (Thomassin *et al.*, 2015), the reason for the severe attenuation of *ΔcpxRA in vivo* was unclear.

In this study, we characterized the *C. rodentium* Cpx regulon in order to identify the mechanisms by which the Cpx response promotes host infection by *C. rodentium*. We used RNA-Seq and stable isotope labeling by amino acids in cell culture (SILAC) approaches in parallel to identify transcripts and proteins, respectively, whose abundance is altered in *C. rodentium ΔcpxRA*. To our knowledge, this is the first direct comparison of the Cpx two-component system's effects on the cellular transcriptome and proteome in the same genetic background in any organism. Follow-up studies with mutants lacking a subset of Cpx-regulated genes identified *degP* and *dsbA* as being particularly important for *C. rodentium*'s ability to infect mice, although Cpx regulation of these genes could not account for the severe attenuation of *C. rodentium ΔcpxRA*. Disruption of disulfide bonding through deletion of *dsbA* or treatment with a chemical reducing agent activated the *C. rodentium* Cpx envelope stress response, suggesting that sensing and correcting envelope protein misfolding may promote A/E pathogenesis.

Results

Characterization of the C. rodentium *Cpx regulon*

To characterize the *C. rodentium* Cpx regulon, we used a dual approach: RNA-Seq was used to identify transcripts whose abundance differs between *C. rodentium* DBS100 and *ΔcpxRA* (Dataset S1), and SILAC was used to characterize changes in whole-cell protein abundance between strains (Dataset S2). SILAC enables the detection of post-transcriptional and post-translational effects that would be missed by RNA-Seq alone, such as changes in protein

abundance mediated by altered protease activity. For both RNA-Seq and SILAC, *C. rodentium* was grown statically in DMEM in 5% CO_2, a condition which is known to activate expression of virulence genes such as those encoding the T3SS (Deng *et al.*, 2003). Using a cutoff of a twofold change in abundance between strains with a false-discovery rate < 0.05, we found 338 transcripts that were differentially expressed by RNA-Seq (207 transcripts more abundant in wild-type than in *ΔcpxRA* and 131 more abundant in *ΔcpxRA* than in wild-type; Dataset S3); by SILAC, we found 19 proteins that were differentially expressed (8 proteins more abundant in wild-type than in *ΔcpxRA*, and 11 more abundant in *ΔcpxRA* than in wild-type; Dataset S3). A comparison of the RNA-Seq and SILAC hits revealed that, while five out of eight proteins positively regulated at least twofold by CpxAR (i.e. more abundant in wild-type than in *ΔcpxRA*) were also upregulated at least twofold at the transcript level in the RNA-Seq results (Figure 1A), only three of 11 proteins negatively regulated at least twofold by CpxAR (i.e. more abundant in *ΔcpxRA* than in wild-type) were also downregulated at least twofold at the transcript level (Figure 1B). These results suggest that the post-transcriptional/post-translational effects mediated by CpxAR may primarily act to decrease protein abundance.

Many of the transcripts/proteins that are more abundant in DBS100 than in *ΔcpxRA* represent envelope-localized protein folding and turnover factors (Table 1). These include genes known to be Cpx-activated in *E. coli*, including those encoding the chaperone and regulator of the Cpx response CpxP, the modulator of proteolysis YccA, the endoprotease HtpX, the chaperone Spy, the peptidyl-prolyl cis-trans isomerase PpiA, and the disulfide bond isomerase DsbA (Vogt and Raivio, 2012). In addition, a number of genes/proteins not previously linked to the Cpx response in *E. coli* were found to be positively regulated by CpxAR in *C. rodentium*, including the protease PtrA and the serine protease inhibitor ecotin. The protease/chaperone DegP, which is a well-characterized Cpx regulon member in *E. coli*, did not pass the 2-fold cutoff in either the RNA-Seq or the SILAC screen (Table 1; Datasets S1 and S2); however, both the transcript and the protein were present at significantly higher levels in DBS100 than *ΔcpxRA* (FDR < 0.05). By RT-qPCR, we confirmed that transcripts for *cpxP*, *yccA*, *eco*, *spy*, and *ppiA* were significantly more abundant in DBS100 than in *ΔcpxRA* (P<0.05, Figure 2A); transcripts for *degP* and *dsbA* were also more abundant in wild-type *C. rodentium*, but the difference between strains was not significant after correction for multiple comparisons (Figure 2A). All of these genes were expressed at a similar level in *ΔcpxR* and *ΔcpxA* single mutants as in the

ΔcpxRA double mutant (Figure S1A-G), suggesting that mutation of either *cpxR* or *cpxA* is sufficient to inactivate the pathway. Single-copy chromosomal complementation of the *ΔcpxRA*, *ΔcpxR*, and *ΔcpxA* mutations restored expression of these genes to their wild-type levels (Figure S1A-G).

RNA-Seq showed that genes encoding several pilus components were also differentially expressed in the *ΔcpxRA* mutant. The *kfcCDEFG* transcript encoding a K99-type chaperone-usher pilus was less than half as abundant in DBS100 as in *ΔcpxRA* (Table 1). Although not every protein encoded in this operon was detected by SILAC, KfcC was also less abundant in DBS100 at the protein level (Table 1; Dataset S2). Downregulation of *kfcC* by the Cpx response was confirmed by RT-qPCR (Figure 2B; expression in *ΔcpxR* and *ΔcpxA* and complemented strains shown in Figure S1H).

Numerous T3S-related genes and proteins were found to be differentially expressed in *ΔcpxRA* by both RNA-Seq and SILAC (Table 1). Several non-LEE encoded effectors were found to be expressed at higher levels in the *ΔcpxRA* mutant by RNA-Seq (*nleB1*, *nleG1*, *nleE*, *espK*, *nleC*, *nleG8*, *nleG7*, *espX7*, *espM3*, and *espS*); although not all of these proteins were detectable by SILAC, those that were detectable (NleB1, NleG1, NleE, NleC, EspX7, and EspS) were generally also found to have higher protein abundance in *ΔcpxRA*. Expression of *nleB1*, the most downregulated non-LEE encoded effector gene in wild-type *C. rodentium* when compared with the *ΔcpxRA* mutant according to RNA-Seq, was further analyzed by RT-qPCR. The latter confirmed that the *nleB1* transcript is approximately twofold less abundant in wild-type *C. rodentium* than in the *ΔcpxRA* mutant (Figures 2C and S1I). Interestingly, no LEE-encoded transcripts were found to be differentially expressed by RNA-Seq; however, the LEE-encoded T3SS translocator protein EspB was found to be greater than twofold more abundant in *ΔcpxRA* by SILAC (Table 1). Using RT-qPCR, we confirmed that the *espB* transcript was equally abundant in both strains (Figures 2C and S1J). Western blotting showed that the EspB protein was more abundant in whole cell lysates of the *ΔcpxR* and *ΔcpxA* mutants (2.3-fold and 1.4-fold higher than the wild-type level, respectively), although increased cellular abundance of EspB was not consistently observed in the *ΔcpxRA* mutant itself (Figure 2D). The abundance of EspB secreted into the culture supernatant did not differ between wild-type and *cpx* mutant strains, nor did abundance of the other major secreted proteins, EspA and EspD (Figure S2). These results suggest that the *C. rodentium* Cpx response negatively regulates expression of T3S-related genes

in two separate ways: the non-LEE encoded effectors appear to be repressed primarily at the transcriptional level, while the LEE-encoded protein EspB may be repressed at the post-transcriptional or post-translational level.

RT-qPCR was also performed to confirm differential expression of several additional genes belonging to other functional categories. By RNA-Seq and SILAC, expression of *rdoA* was found to be significantly higher in wild-type *C. rodentium* (Table 1). RdoA is a serine/threonine protein kinase involved in regulating programmed cell death (Dorsey-Oresto *et al.*, 2013); *rdoA* is encoded immediately upstream of *dsbA* and the two genes are known to be co-transcribed from a Cpx-activated promoter in *E. coli* (Pogliano *et al.*, 1997). RT-qPCR analysis confirmed that *rdoA* is modestly but reproducibly positively regulated by CpxAR in *C. rodentium* as well (Figures 2E and S1K). Four genes comprising a putative operon (ROD_17451, ROD_17461, ROD_17471, and ROD_17481) encode several of the transcripts and proteins that were most strongly activated by CpxAR in both the RNA-Seq and SILAC datasets (Table 1). ROD_17451 is homologous to *E. coli* gene of unknown function *yciG*; ROD_17461 and ROD_17471 both contain putative ruberythrin/ferritin-like metal-binding domains, and ROD_17481 is a putative Mn-containing catalase. RT-qPCR confirmed that all four genes are positively regulated by CpxAR in *C. rodentium* (Figures 2E and S1L). Finally, several proteins involved in 1,2-propanediol utilization (PduE, PduB, PduJ) were found by SILAC to be repressed by CpxAR in *C. rodentium* (~3-fold less abundant in wild-type than *ΔcpxRA*; Table 1), yet the RNA-Seq results indicate that the transcripts encoding these proteins were present at similar levels in the two strains. Three additional Pdu proteins (PduK, PduA, and PduD) were also found to be downregulated more than twofold by SILAC but not by RNA-Seq; however, since these proteins were identified in only one of three SILAC replicates, they were not considered statistically significant (Dataset S2). By RT-qPCR, we confirmed that the *pduJ* transcript is not differentially expressed in *ΔcpxRA* compared to DBS100 (Figures 2E and S1M), suggesting that the Pdu proteins are repressed by CpxAR at the post-transcriptional or post-translational level.

Identification of Cpx-regulated genes required for host infection

Having characterized the *C. rodentium* Cpx regulon, we next aimed to determine whether any of the Cpx-regulated genes play a role in host infection. To this end, we generated

C. rodentium mutants carrying deletions in individual genes or operons positively regulated by CpxAR. Since the large number of Cpx-regulated genes precluded analysis of every Cpx regulon member, we prioritized genes that are known to be directly regulated by CpxR in *E. coli* (*cpxP*, *degP*, *dsbA*, *ppiA*, *spy*, *yccA*) or that were strongly upregulated by CpxAR in the RNA-Seq or SILAC experiments (ROD_17451-81 putative operon, *eco*).

Prior to performing infection studies, we performed preliminary characterization of the mutants *in vitro*. All of the mutants grew at a rate comparable to wild-type *C. rodentium* in both rich medium (LB) and conditions known to stimulate expression of virulence genes (DMEM with 5% CO_2) (Figure S3). Most of the Cpx regulon mutants had secreted protein profiles that were similar to that of wild-type strain DBS100; however, the supernatant of the *ΔdegP* mutant contained large amounts of non-type III-secreted proteins, while the *ΔdsbA* mutant supernatant contained reduced amounts of EspA, EspB, and EspD (Figure 3). Western blotting of secreted proteins with an α-EspB antibody confirmed reduced levels of EspB in the *ΔdsbA* culture supernatant and also revealed that, in spite of the increased quantity of protein in the *ΔdegP* supernatant, the amount of EspB secreted by this strain was actually less than the wild-type level (Figure 3). Similar phenotypes have been observed in EPEC *ΔdegP* and *ΔdsbA* mutants (Miki *et al.*, 2008; MacRitchie *et al.*, 2012), suggesting that these proteins play a conserved role in envelope integrity and assembly or function of the T3S machinery, respectively. Single-copy chromosomal complementation of the *ΔdegP* and *ΔdsbA* mutants completely restored the aberrant secreted protein profiles to match the wild-type phenotype (Figure S4A).

We next assessed the ability of the *C. rodentium* mutants to colonize and cause lethal infection in C3H/HeJ mice. In agreement with previous studies, we found that the *ΔcpxRA* mutant was attenuated in this mouse model (Figure 4A). However, in our experiments, the *ΔcpxRA* mutant was still able to cause lethal infection in about half of the mice, in contrast to the 100% survival previously reported (Thomassin *et al.*, 2015; Thomassin *et al.*, 2017). The reason for the differing results is unknown, since all C3H/HeJ mice originated from the same supplier. However, *C. rodentium* infection outcomes are known to be sensitive to alterations to the gut microbiota (Willing *et al.*, 2011; Wlodarska *et al.*, 2011; Kamada *et al.*, 2012), and therefore differences in mouse chow or other environmental parameters that affect gut microbiota composition between animal facilities might affect the virulence of *C. rodentium* mutants. The *ΔcpxR* and *ΔcpxA* single mutants were attenuated to a similar degree as the *ΔcpxRA* double

mutant (Figure S5), as expected based on the similarity in gene expression between these three strains (Figure S1). The majority of the Cpx regulon mutants were indistinguishable from wild-type *C. rodentium* in their ability to cause lethal infection (Figure 4A); however, the *ΔdegP* and *ΔdsbA* mutants did not kill any of the infected animals. Virulence was fully restored to the *ΔdegP* and *ΔdsbA* mutants by single-copy chromosomal complementation (Figures S4B and S4C). All of the attenuated mutants (*ΔcpxRA*, *ΔdegP*, and *ΔdsbA*) were able to colonize the mouse gut, as assessed by fecal shedding of *C. rodentium*, albeit at a level 1 to 2 logs lower than the wild-type strain (Figure 4B). Thus, among the Cpx regulon members tested, DegP and DsbA are most important for the ability of *C. rodentium* to colonize and cause infection in C3H/HeJ mice.

Cpx regulation of degP *and* dsbA *does not fully account for CpxAR's role in virulence*

Since the *ΔdegP* and *ΔdsbA* mutants were essentially avirulent in C3H/HeJ mice (Figure 4), we hypothesized that the decreased colonization and virulence of the *ΔcpxRA* mutant could result from its reduced expression of *degP* and *dsbA*. To test this hypothesis, we sought to identify and mutate the CpxR binding sites upstream of *degP* and *dsbA*, leaving the genes and promoters otherwise intact.

The location of the CpxR binding site in the *E. coli degP* promoter has been experimentally identified (Pogliano *et al.*, 1997), and a sequence alignment shows that the CpxR binding motifs are conserved in the *C. rodentium degP* promoter (Figure 5A). In order to verify that this region is responsible for CpxAR regulation of the *degP* promoter in *C. rodentium*, we cloned the *degP* promoter into the *luxCDABE* transcriptional reporter plasmid pNLP10. We then measured activity of the wild-type *degP* reporter as well as a reporter with a 25-bp deletion encompassing the CpxR boxes (as shown in Figure 5A) in both wild-type and *ΔcpxRA* strains of *C. rodentium.* Activity of the wild-type *degP* promoter was approximately four-fold higher in wild-type *C. rodentium* than in *ΔcpxRA* (Figure 5B); however, activity of the $P_{degP\Delta CpxR}$ reporter did not differ between DBS100 and *ΔcpxRA*, suggesting that the deleted region contained the CpxR binding sites. To confirm that no other region of the *degP* promoter is required for CpxR regulation, we generated a chromosomal deletion of the same 25 bp in the *degP* promoter and measured *degP* transcript abundance by RT-qPCR. While introduction of the *ΔcpxRA* deletion into *C. rodentium* with a wild-type *degP* promoter caused a significant decrease in *degP* transcript abundance, no change in *degP* transcript abundance was seen when the *ΔcpxRA* allele

was introduced into the $P_{degP\Delta CpxR}$ background (Figure 5C). These results indicate that the same region of the *degP* promoter is responsible for CpxR activation in both *E. coli* and *C. rodentium*.

In *E. coli*, *dsbA* is expressed both from a proximal promoter directly upstream of *dsbA* and from a distal promoter located upstream of *rdoA*, the gene immediately upstream of *dsbA* (Belin and Boquet, 1994); only the distal promoter is subject to CpxR regulation (Pogliano *et al.*, 1997). To assess the effect of CpxAR on the *rdoA* and *dsbA* promoters in *C. rodentium*, the two promoter regions were cloned into medium-copy luminescence reporter vector pJW15. Activity of the *rdoA* reporter was significantly higher in wild-type *C. rodentium* than in *ΔcpxRA*, while activity of the *dsbA* reporter was actually slightly higher in the *ΔcpxRA* mutant (Figure 6A), indicating that CpxR activates *dsbA* expression via the *rdoA* promoter in *C. rodentium*, similarly to *E. coli*. Next, we set out to mutate the *rdoA* promoter in order to abolish Cpx regulation of the *rdoA-dsbA* operon. However, we could not delete the entire CpxR binding region as we did with the *degP* promoter, because: (i) the CpxR binding region in the *rdoA* promoter partially overlaps the coding sequence of the upstream gene ROD_39011 (underlined in Figure 6B) – we therefore needed to ensure that any mutations were synonymous with respect to the ROD_39011 coding sequence; and (ii) deletion of the 3' CpxR box completely abolished *rdoA* promoter activity (data not shown), perhaps due to its proximity to the -35 element (Figure 6B). For this reason, we introduced three point mutations into the first CpxR box as shown in Figure 6B. These point mutations abolished CpxAR regulation of the mutant $P_{rdoAmut}$-*lux* reporter (Figure 6C), although the lower activity of this reporter relative to the wild-type P_{rdoA}-*lux* reporter in the *ΔcpxRA* background suggested that the mutations may have also affected basal promoter activity. However, when the $P_{rdoAmut}$ mutations were introduced into the chromosome, abundance of the *rdoA* and *dsbA* transcripts was not reduced below their levels in the *ΔcpxRA* mutant (Figures 6D and 6E), indicating that the low expression of $P_{rdoAmut}$-*lux* may have been a multicopy artifact.

In order to examine whether Cpx regulation of *degP* and *dsbA* is important for *C. rodentium* host infection, we infected C3H/HeJ mice with *C. rodentium* strains carrying one or both of the $P_{degP\Delta CpxR}$ and $P_{rdoAmut}$ mutations. It is important to note that, although *rdoA* expression is also reduced in the $P_{rdoAmut}$ strain, we assumed that any decrease in virulence would be due to misregulation of *dsbA*, since a *ΔrdoA* mutant was not attenuated in this model (Figure S6). There was no statistically significant difference in mortality between mice infected with wild-type *C. rodentium* and any of the single or double promoter mutants (Figure 7A, $P>0.05$,

Mantel-Cox test with Bonferroni's correction for multiple comparisons). Fecal shedding of the promoter mutants was also indistinguishable from that of wild-type *C. rodentium*, whereas fecal shedding of the attenuated *ΔcpxRA*, *ΔdegP*, and *ΔdsbA* mutants tended to be lower than wild-type throughout the course of infection (Figure 7B). Together, these results indicate that, although *degP* and *dsbA* are essential for *C. rodentium* infection of mice, CpxAR regulation of only these genes does not fully account for the impaired virulence of the *ΔcpxRA* mutant in this infection model.

Disulfide bond disruption is an inducing signal for the C. rodentium *Cpx response*

To further examine the physiological role of the *C. rodentium* Cpx response, we next addressed the question of which signal activates the response. Although it has previously been reported that the *C. rodentium* Cpx response is activated at alkaline pH (Thomassin *et al.*, 2015), the molecular nature of the inducing signal remains unknown. Since the Cpx response is believed to sense protein misfolding in the inner membrane and/or periplasm (Vogt and Raivio, 2012), we examined whether any of our Cpx regulon mutants – many of which lack important periplasmic protein folding and degrading factors – had altered Cpx pathway activity using a *cpxP-lux* transcriptional reporter. Since *cpxP* is the gene that was most strongly activated by CpxAR in *C. rodentium* according to RNA-Seq and RT-qPCR (Table 1, Figure 2A) and is not known to be regulated at the transcriptional level by any regulators other than CpxR in either *C. rodentium* or *E. coli*, activity of the *cpxP-lux* transcriptional reporter is a good proxy for Cpx pathway activity. As expected, we found that the *ΔcpxRA* mutant had dramatically reduced *cpxP-lux* activity compared to the wild-type strain (Figure 8A). In addition, two regulon mutants had *cpxP-lux* activity that was significantly higher than DBS100 ($P<0.0001$). The *C. rodentium ΔcpxP* mutant had an approximate 4-fold increase in *cpxP-lux* activity compared to the wild-type strain (Figure 8A), which is in keeping with the finding that CpxP acts as a negative regulator of Cpx pathway activity in *E. coli* (Raivio *et al.*, 1999). Interestingly, the *ΔdsbA* mutant had even higher *cpxP-lux* activity than the *ΔcpxP* mutant (Figure 8A), suggesting that disruption of disulfide bonding in the envelope could act as an inducing cue for the *C. rodentium* Cpx response. To further examine this idea, we measured the activity of the Cpx pathway in the presence of dithiothreitol (DTT), a chemical reducing agent known to disrupt disulfide bonds in proteins. We found that activity of the *cpxP-lux* reporter increased in the presence of DTT in a dose-dependent manner (Figure 8B),

while activity of several *lux* reporters not regulated by the Cpx response was not increased by DTT (data not shown). These data suggest that disruption of disulfide bonding in envelope proteins may represent a physiological activating cue for the *C. rodentium* Cpx response.

Discussion

C. rodentium harbours 26 two-component systems (2CSs); mutants in only six of these 2CSs are attenuated in the mouse infection model, with *ΔcpxRA* having the largest virulence defect (Thomassin *et al.*, 2017). The main question we set out to answer in this study is why CpxAR is so important for host infection. Using both transcriptomic and proteomic approaches, we found that CpxAR regulates expression of several hundred genes and proteins at both the transcriptional and post-transcriptional/post-translational level (Dataset S3). Numerous envelope-localized chaperones and proteases were positively regulated by CpxAR, while the Kfc pilus, several T3S effectors, and several proteins comprising the propanediol utilization microcompartment were negatively regulated by CpxAR (Table 1; Figure 2). Among these Cpx-regulated genes, we were able to identify two genes, encoding the major periplasmic protease DegP and the disulfide bond oxidoreductase DsbA, that are essential for *C. rodentium* virulence in C3H/HeJ mice (Figure 4). Therefore, we propose that ensuring correct folding of envelope proteins is a major physiological role of the Cpx response in *C. rodentium* that is likely important during host infection.

Our results are consistent with a previous study that found that a *C. rodentium degP* mutant had a reduced ability to colonize C57BL/6 mice (Cheng *et al.*, 2012). One possible reason for the virulence defect of the *ΔdegP* and *ΔdsbA* mutants could be related to problems with assembly of the T3SS. We noticed that the *ΔdegP* and *ΔdsbA* mutants both had aberrant T3S profiles (Figure 3), similar to previous findings in EPEC (MacRitchie *et al.*, 2012). Miki *et al.* (2008) showed that DsbA catalyzes disulfide bond formation in EPEC EscC, the outer membrane secretin component of the T3SS, and that this disulfide bond is likely formed between cysteine residues 136 and 155. Given that both of these cysteines are conserved in *C. rodentium* EscC (data not shown), it is likely that DsbA performs a similar role in *C. rodentium*. In addition to facilitating proper biogenesis of the T3SS, DegP and DsbA also promote biogenesis of the bundle-forming pilus in EPEC (Zhang and Donnenberg, 1996; Vogt *et al.*, 2010; Humphries *et al.*, 2010). Since several pili reportedly contribute to *C. rodentium* colonization of the mouse gut

(Mundy *et al.*, 2003; Hart *et al.*, 2008; Caballero-Flores *et al.*, 2015), proper folding of these proteins could be another important role for DegP and DsbA *in vivo*.

Despite the fact that the *ΔdegP* and *ΔdsbA* deletion mutants were avirulent in C3H/HeJ mice (Figure 4), mutation of the CpxR boxes located upstream of the two genes did not significantly reduce virulence compared to wild-type *C. rodentium* (Figure 7). This discrepancy can likely be attributed to the relatively weak activation of these two genes by CpxAR. Although expression of *degP* and *dsbA* is reduced by deletion of *cpxRA* (Table 1; Figures 2A, 5, and 6) or by mutation of the CpxR box in their promoter regions (Figures 5 and 6), the decrease in expression is around twofold or less. Therefore, even in the absence of Cpx activation, basal expression of *degP* and *dsbA* may be sufficient for proper protein folding *in vivo*. Alternatively, or in addition, other signaling pathways may upregulate these genes *in vivo*. This finding leaves open the question of why the *ΔcpxRA* mutant is attenuated. One possibility is that there remains one or more Cpx-regulated genes that are essential for host infection, but whose contribution to virulence was not examined in this study. Although we did delete several of the most strongly Cpx-regulated genes (*cpxP*, *yccA*, *eco*, ROD_17451-81) and found the mutants to be fully virulent, there remain a number of Cpx-regulated genes whose contribution has not yet been examined. Another possible explanation for the attenuation of the *ΔcpxRA* mutant could be the cumulative effect of misregulation of numerous envelope protein folding factors. Although the decreased expression of *degP* and *dsbA* in the *ΔcpxRA* mutant is not sufficient to cause attenuation (Figure 7), expression of several additional proteases, protease regulators, and chaperones is also reduced in this strain (Table 1, Figure 2A). Perhaps these proteases and chaperones can compensate for reduced expression of *degP* and *dsbA* in an otherwise wild-type background, but not at their reduced levels in the *ΔcpxRA* mutant.

Another intriguing possibility is that repression of target genes by CpxR is important *in vivo*. We found that CpxAR downregulates expression of the *kfc* pilus gene cluster, numerous T3S effectors, and the Pdu propanediol utilization microcompartment proteins (Table 1, Figure 2). All of these proteins are structural components of, or require secretion by, large macromolecular complexes that require substantial cellular resources to produce. Thus, overexpression of all of these proteins might confer a growth disadvantage *in vivo*. In addition, overexpression of virulence-related proteins can have other detrimental effects. For example, deletion of *cpxR* in UPEC strain UTI89 causes overexpression of the hemolysin HlyA

(Nagamatsu *et al.*, 2015). UTI89 *ΔcpxR* has a reduced ability to colonize the bladder of C3H/HeN mice, which is likely the result of this strain's increased ability to induce exfoliation of infected urothelial cells (Nagamatsu *et al.*, 2015). Importantly, the virulence defect of the *ΔcpxR* mutant can be attributed to its increased expression of *hlyA*, since deletion of *hlyA* in the *ΔcpxR* background reduces urothelial cell exfoliation and restores wild-type colonization ability (Nagamatsu *et al.*, 2015). Thus, it is possible that increased expression of virulence proteins such as T3S effectors in *C. rodentium ΔcpxRA* is detrimental to host colonization, perhaps by more strongly inducing host defense pathways.

We found that Cpx repression of several protein complexes in *C. rodentium* appears to happen partially or entirely post-transcriptionally. Although numerous non-LEE-encoded T3S effectors appeared to be repressed by CpxAR at the transcriptional level (e.g. *nleB1*; Table 1 and Figure 2C), none of the genes encoded in the LEE were differentially expressed between DBS100 and *ΔcpxRA* at the transcript level according to our RNA-Seq data (Table 1), and we confirmed by RT-qPCR that *espB* transcripts were equally abundant in DBS100 and *ΔcpxRA* (Figure 2C). However, we observed by SILAC and confirmed by Western blotting that the T3S translocator protein EspB was more abundant in *Δcpx* cell pellets than in the wild-type strain (Table 1; Figure 2D). In addition, several Pdu proteins involved in formation of the 1,2-propanediol microcompartment were found to be more abundant in *ΔcpxRA* by SILAC (Table 1), even though their transcripts were not differentially expressed according to RNA-Seq and RT-qPCR (Figure 2E). Several other examples of post-transcriptional effects mediated by CpxAR have been described in other organisms. For example, deletion of *cpxA* in EHEC (which activates the Cpx pathway due to loss of CpxA's phosphatase activity) causes decreased expression of LEE-encoded T3SS proteins such as EspA, EspB, and EspD (De la Cruz *et al.*, 2016). The repression of T3SS expression in EHEC *ΔcpxA* is dependent on the presence of Lon protease, suggesting that activation of the Cpx response causes Lon to degrade a regulator required for T3SS gene expression (De la Cruz *et al.*, 2016). Lon is also required for Cpx-mediated repression of T3SS-1 expression in *Salmonella* Typhimurium; in this case, activation of the Cpx response causes Lon to degrade the regulatory protein HilD (De la Cruz *et al.*, 2015). It is currently unknown whether Lon might be responsible for the post-transcriptional repression of EspB and the Pdu proteins in *C. rodentium*. However, if Lon is involved, the mechanism likely differs from that in EHEC, since Cpx activation in EHEC causes reduced transcription of

LEE-encoded genes including *espA*, *ler*, and *tir* (De la Cruz *et al.*, 2016), whereas we observed differences in EspB protein abundance but not *espB* transcript abundance in *C. rodentium* *ΔcpxRA* (Table 1, Figure 2). In any case, these findings together point to a previously underappreciated ability of the Cpx response to alter the cellular proteome through post-transcriptional mechanisms.

A major outstanding question about the physiological role of the Cpx response pertains to the nature of its inducing cue(s). Here, we found that deletion of *dsbA* caused activation of the Cpx response in *C. rodentium* (Figure 8A). Since treating cells with the chemical reductant DTT also activated CpxAR (Figure 8B), reduction of disulfide bonds in envelope proteins may represent a cue for Cpx activation in *C. rodentium*. It is currently unknown how CpxAR might sense problems with disulfide bond formation in envelope proteins. Neither CpxA (the sensor kinase) nor CpxP (the periplasmic inhibitory protein) contain any cysteine residues in *C. rodentium* (data not shown); thus, they cannot directly sense disruption of disulfide bonding. However, the lipoprotein NlpE, which acts as an accessory regulator capable of activating the Cpx response in *E. coli* (Snyder *et al.*, 1995), is capable of forming an intramolecular disulfide bond (Hirano *et al.*, 2007). Since the redox-active cysteine residues in *E. coli* NlpE are conserved in *C. rodentium* (data not shown), this could represent a potential mechanism for Cpx sensing of disulfide bond disruption. It is also unclear whether disulfide bond disruption is a physiologically relevant inducer of the Cpx response during *C. rodentium* growth in the mouse gut, where Thomassin and colleagues (2015) previously showed that the Cpx-activated genes *cpxR*, *cpxA*, and *cpxP* are expressed. Several host-derived and microbiota-derived reducing agents are known to be present in the gut; for example, human thioredoxin is expressed in the gut mucosa and is responsible for reducing disulfide bonds in the antimicrobial peptide β-defensin 1 (Schroeder *et al.*, 2011). Further research will be required to determine whether reduction of disulfide bonds contributes to activity of the *C. rodentium* Cpx response *in vivo*.

In summary, our analysis of the *C. rodentium* Cpx regulon demonstrates the conserved role of the Cpx envelope stress response in enterobacteria, with envelope-localized chaperones and proteases being Cpx-activated and envelope protein complexes such as pili and secretion systems being Cpx-repressed in numerous species. Interestingly, the Cpx response appears to be important for gut colonization by pathogens and commensals alike, since a *ΔcpxR* mutant of mouse commensal *E. coli* strain MP1 has a severe colonization defect (Lasaro *et al.*, 2014).

Together, these results highlight the importance of envelope protein biogenesis for the ability of Gram-negative bacteria to interact with their hosts.

Experimental Procedures

Bacterial strains and growth conditions

Bacterial strains and plasmids used in this study are listed in Table S1. Unless otherwise stated, all strains were grown in lysogeny broth (LB; 10 g l^{-1} tryptone, 5 g l^{-1} yeast extract, 10 g l^{-1} NaCl) at 37ºC with aeration at 225 rpm or on LB agar at 37ºC. Antibiotics and supplements were used when necessary at the following concentrations: ampicillin, 100 µg ml^{-1}; chloramphenicol, 30 µg ml^{-1}; kanamycin, 50 µg ml^{-1}; diaminopimelic acid (DAP), 0.3 mM.

RNA-Seq

Strains were grown overnight in biological triplicate cultures in 5 ml of LB at 37˚C, aerated at 220 rpm, and then diluted in LB to an OD_{600} of 1.0. One ml of each dilution was pelleted at 2300 × g for 5 min at room temperature and resuspended in 20 ml of prewarmed DMEM (HG) (Caisson Labs, Cat. Number: DML07), to which arginine and lysine were added to final concentrations of 0.2 mM and 0.8 mM, respectively. Cultures were incubated for 4.5 hours at 37°C in a 5% CO_2 incubator, statically. RNA was isolated from these cultures using the MasterPure RNA purification kit (Epicentre) following the manufacturer's instructions and including a further 2 Units of DNase I (Invitrogen) treatment at 37˚C for 30 min. Final RNA samples were resuspended in 50 µl of nuclease-free water and reverse transcription and real time qPCR were done to verify DNA depletion using primers specific for the *dnaQ* gene (Table S2). 20 µg of RNA were submitted for sample preparation and RNA-Seq analysis by GENEWIZ (Plainfield, NJ). Single read sequencing was done on an Illumina HiSeq 2500 platform. Reads were mapped to the *C. rodentium* ICC168 reference genome (NC_013716, NC_013717, NC_013718, and NC_013719) using EDGE-pro (Magoc *et al.*, 2013) and differentially expressed genes were identified using DESeq2 (Love *et al.*, 2014), based on a > 2 fold or < 0.5 fold change in the wild-type DBS100 strain as compared to the *ΔcpxRA* mutant with a Benjamini-Hochberg-adjusted *P* value < 0.05.

Stable isotope labeling by amino acids (SILAC)

SILAC was performed similarly as previously described (Brown *et al.*, 2014). To ensure efficient isotopic labelling of bacterial proteins, a Lys^- Arg^- auxotroph (DBS100 *ΔlysA ΔargH*) was used as "wild-type" *C. rodentium* for these experiments (Deng *et al.*, 2010). Briefly, bacteria were grown in LB overnight at 220 rpm and 37°C before being used to inoculate defined lysogeny broth (dLB) including isotope-labeled arginine (0.2 mM) and lysine (0.8 mM) at an inoculation ratio of 1:10000. Labeling with L-arginine and L-lysine ("light" label (L), *C. rodentium ΔlysA ΔargH ΔcpxRA*) or L-[$^{13}C_6$]arginine and L-[$^{2}H_4$]lysine ("heavy" label (H), "wild-type" *C. rodentium ΔlysA ΔargH*) was performed under shaking conditions overnight at 220 rpm and 37˚C.

Sample preparation for whole proteome analysis

Antibiotic-, serum-, arginine- and lysine-free Dulbecco's modified Eagle medium (DMEM, Caisson Laboratories Inc.) was supplemented with L-arginine and L-lysine or L-[$^{13}C_6$]arginine and L-[$^{2}H_4$]lysine and prewarmed at 5% (v/v) CO_2 and 37˚C overnight. SILAC-labeled bacteria corresponding to a bacterial load of a 1 ml culture with OD_{600} of 1 were centrifuged at 2300 × g for 5 min at room temperature and resuspended in 20 ml prewarmed DMEM in biological triplicate cultures. The cultures were incubated standing in a 10 cm petri dish at 5% (v/v) CO_2 and 37˚C for 4.5 h. Bacteria were pelleted at 3000 × g and 4˚C for 10 min, washed once in ice-cold phosphate-buffered saline (PBS), resuspended in 50 mM ammonium bicarbonate and 150 mM sodium deoxycholate and incubated at 99˚C under constant agitation for 15 min. $MgCl_2$ was added to a final concentration of 1.5 mM and DNA digestion was achieved by Benzonase endonuclease (Santa Cruz Biotechnology) at room temperature for 30 min. Subsequent to centrifugation at 16000 × g and room temperature for 1 min, the protein concentration was determined by bicinchoninic acid assay (Thermo Scientific Pierce) and the soluble lysate of light and heavy labeled bacteria were combined at a ratio of 1:1. Proteins were reduced with 10 mM dithiothreitol (DTT) at room temperature for 30 min. Samples were then alkylated with 55 mM iodoacetamide in the dark at room temperature for 20 min, sequence grade trypsin (Promega) was added, and protein digestion was achieved under shaking conditions at 37˚C for 16 h. Prior to basic reverse-phase fractionation, peptides were desalted using C18 StAGE Tips (Rappsilber *et al.*, 2007).

Basic reverse-phase fractionation

Basic reverse-phase fractionation was undertaken according to the protocol of Udeshi *et al* with minor modifications (Udeshi *et al.*, 2013). Briefly, peptides were separated using an 1100 series HPLC instrument with a Zorbax Extend C_{18} column (1.0 by 50 mm, 3.5 µm; Agilent) at a flow rate of 100 µl/min. The following gradient was run: initial 5 min from 100% buffer A (5 mM ammonium formate, 2% acetonitrile, pH 10) to 6% buffer B (5 mM ammonium formate, 90% acetonitrile, pH 10), then in 2 min to 8% buffer B, followed by an increase to 27% buffer B in 38 min, to 31% B in 4 min, to 39% B in 4 min, to 60% B in 7 min, and completion with a 4-min run at 100% buffer B and a 26-min gradient back to 100% buffer A. Fractions of 100 µl were collected in a 96-well plate with every eighth fraction combined to generate a total of eight fractions that were concentrated by vacuum centrifugation and subjected to MS analysis.

Liquid chromatography-tandem MS (MS/MS) analysis

Purified peptides were resuspended in buffer A* (0.1% TFA) and separated on an EASY-nLC1000 system coupled to an LTQ-Orbitrap Velos (Thermo Scientific). Briefly, samples were loaded directly onto an in-house-packed 30-cm, 75-µm-inner-diameter, 360-µm-outer-diameter Reprosil-Pur C_{18} AQ 3 µm column (Dr. Maisch, Ammerbuch-Entringen, Germany). Reverse-phase analytical separation was performed at 350 nl/min over a 180-min gradient by altering the buffer composition from 100% buffer A (0.1% formic acid, 2% acetonitrile) with buffer B (0.1% formic acid, 80% acetonitrile) from 0 to 32% in 150 min, from 32 to 40% in the next 5 min, increasing it to 100% in 2.5 min, holding it at 100% for 2.5 min, and then dropping it to 0% for another 20 min. The LTQ-Orbitrap Velos was operated with Xcalibur v2.2 (Thermo Scientific) at a capillary temperature of 275°C with data-dependent acquisition using collision-induced dissociation (CID) MS/MS (normalized collision energy (NCE), 35%; activation Q, 0.25; activation time, 10 ms; automated gain control (AGC) at 4×10^4).

MS data analysis

MS data were processed with MaxQuant (v1.5.2.8) (Cox and Mann, 2008). Database searching was carried out against the reference *C. rodentium* ICC168 proteome (downloaded from UniProt on 22 March 2015; 4,775 proteins) with the following search parameters: carbamidomethylation

of cysteine as a fixed modification, oxidation of methionine, acetylation of protein N-terminal trypsin/P cleavage with a maximum of two missed cleavages. A multiplicity of two was used, with each multiplicity denoting one of the SILAC amino acid combinations (light and heavy respectively). The precursor mass tolerance was set to 6 parts-per-million (ppm) and MS/MS tolerance 0.5 Da for LTQ-velos data with a maximum false discovery rate of 1.0% set for protein identifications. To enhance the identification of peptides between fractions and replicates, the Match between Runs option was enabled with a precursor match window set to 2 min and an alignment window of 10 min. The resulting protein group output was processed within the Perseus (v1.5.0.9) (Tyanova *et al.*, 2015) analysis environment to remove reverse matches and common protein contaminants. Normalized, log2 transformed H/L SILAC ratios (wild-type *Citrobacter rodentium* versus *Citrobacter rodentium ΔcpxRA*) were calculated. Proteins were considered regulated if they showed an average fold change in abundance of at least 2-fold from at least two out of three biological replicates and passed the statistical analysis with multiple hypothesis corrections using a Benjamini–Hochberg procedure with FDR of 0.05. The calculation of a protein SILAC ratio by the MaxQuant software required a minimum of two unique peptides to be identified. Some proteins were differentially expressed according to RNA-Seq data, detected in mass spectrometry but no SILAC ratios were determined by the MaxQuant software since less than two unique peptides were identified for these particular proteins. Thus, for reasons of better comparability between both data sets, not protein- but peptide-based SILAC ratios were considered for this particular set of proteins. All mass spectrometry proteomics data have been deposited to the ProteomeXchange Consortium via the PRIDE partner repository with the dataset identifier PXD009049 (Vizcaíno *et al.*, 2016).

Reverse transcriptase quantitative PCR (RT-qPCR)

For RNA extraction, strains were first cultured overnight in LB, then subcultured into 20 ml of prewarmed Dulbecco's Modified Eagles Medium (DMEM) (HyClone cat. no. SH30243.01) in a 100 mm Petri dish at a starting OD_{600} of 0.05. Cultures were incubated for 4.5 h at 37ºC in a static incubator with 5% CO_2. RNA was extracted from 500 µl of culture using RNAprotect Bacteria Reagent (Qiagen) followed by the GeneJET RNA Purification Kit (Thermo Fisher Scientific). Contaminating genomic DNA was removed from 2-µg aliquots of purified RNA using the TURBO DNA-free Kit (Thermo Fisher Scientific), followed by reverse transcription

with the QuantiTect Reverse Transcription Kit (Qiagen). RT-qPCR was performed using the QuantiTect SYBR Green PCR Kit (Qiagen) on an Applied Biosystems 7500 Fast Real-Time PCR System, using the $\Delta\Delta C_T$ relative quantitation method with *dnaQ* (which was experimentally verified to be expressed at equal levels in the wild-type and *ΔcpxRA* strains; data not shown) as the endogenous control. Primers used for RT-qPCR are listed in Table S2; the efficiency of all primer pairs was verified to be within the range of 90-110% (data not shown). No-template and no-reverse transcriptase controls were included in each RT-qPCR plate to confirm the absence of primer dimer and contaminating genomic DNA, respectively. All RT-qPCR data represent biological triplicate cultures.

Western blot analysis

C. rodentium strains were cultured as described above for RT-qPCR analysis. After 4.5 h growth in DMEM, 1 ml of each culture was pelleted and resuspended in 75 µl 2× sample buffer [125 mM Tris (pH 6.8), 20% glycerol, 10% β-mercaptoethanol, 6% sodium dodecyl sulfate, 0.2% bromophenol blue]. Electrophoresis and Western blotting to detect EspB and DnaK were performed as previously described (Deng *et al.*, 2004). Quantification of proteins in Western blots was performed using the Image Lab software on a ChemiDoc gel imager (Bio-Rad).

Strain and plasmid construction

All *C. rodentium* deletion mutants were generated by allelic exchange. Briefly, in-frame deletion constructs for each gene were generated by overlap-extension PCR (Ho *et al.*, 1989) using the UpF-UpR and DnF-DnR primers listed in Table S2. Overlap PCR products were restriction digested and ligated into pUC18. All inserts were confirmed by Sanger sequencing, then subcloned into suicide vector pRE112 (Edwards *et al.*, 1998). Suicide plasmids were transferred into *C. rodentium* by biparental mating using MFDPir as the donor (Ferrières *et al.*, 2010) with transconjugants selected on LB chloramphenicol plates. Loss of the pRE112 plasmid from the *C. rodentium* chromosome was subsequently selected for by growth on LB agar with 5% sucrose. Sucrose-resistant, chloramphenicol-sensitive colonies were screened for presence of the intended deletion by PCR.

Single-copy, chromosomally complemented strains were constructed using the mini-Tn7 system (Choi *et al.*, 2005). Briefly, the chloramphenicol resistance cassette from pKD3

(Datsenko and Wanner, 2000) was amplified using primers P1_cat and P2_cat (Table S2) and cloned into the mini-Tn7 transposon in pUC18R6KT-mini-Tn7T (Choi *et al.*, 2005). Genes to be complemented, driven by their native promoters, were amplified using primers listed in Table S2 and cloned into the *Kpn*I and *XhoI* sites in pUC18R6KT-mini-Tn7T-Cm. The *ΔcpxA* mutant was complemented using *cpxRA* since *cpxA* expression is driven by the promoter upstream of *cpxR*. Transposon-containing plasmids were transferred into target strains by triparental mating using MFDPir as the donor strain and the pTNS2 transposase-encoding plasmid (Choi *et al.*, 2005). Insertion of the mini-Tn7 element into the correct chromosomal location was verified by PCR using the primers PTn7R and PglmS-down_Citro (Table S2).

In order to construct DBS100 $P_{degP\Delta CpxR}$, $P_{rdoAmut}$, and the related *lux* reporters pNLP10$P_{degP\Delta CpxR}$ and pJW15$P_{rdoAmut}$, we used overlap-extension PCR (with primers listed in Table S2) to generate PCR products containing the desired mutation with ~1 kb of flanking DNA on each side. The overlap PCR products were then cloned into pUC18 and sequenced. To generate chromosomal mutations, the inserts were subcloned into pRE112 and transferred into *C. rodentium* as described above. To generate *lux* reporters, the mutated promoter regions were amplified from the pUC18 plasmids using primers PdegPF/PdegPR and PrdoAF/PrdoAR (Table S2); PCR products were then restriction digested and ligated into pNLP10 and pJW15, respectively.

T3S assay

Proteins secreted by *C. rodentium* during growth in DMEM were precipitated using trichloroacetic acid (TCA) and analyzed by SDS-PAGE and Coomassie staining as previously described (Deng *et al.*, 2003). 2 µg of purified bovine serum albumin (BSA) was added to each collected supernatant prior to addition of TCA to aid in protein precipitation.

Mouse infections

All animal experiments were performed in accordance with the guidelines of the Canadian Council on Animal Care and the University of British Columbia (UBC) Animal Care Committee (certificate A12-0238). Mice were ordered from Jackson Laboratory (Bar Harbor, ME) and maintained in a specific pathogen-free facility at UBC. Seven-week-old female C3H/HeJ mice were orally gavaged with 100 µl of overnight culture of *C. rodentium* grown in LB (containing

~3×10^8 CFU of bacteria as confirmed by retrospective plating). Mice were monitored daily for weight loss and clinical symptoms. *C. rodentium* shedding was monitored by plating dilutions of fecal samples on MacConkey agar every two days throughout the 30-day infection. Upon reaching the humane endpoint (weight loss of 20%; or any one of: bloody diarrhea, severe hunching, severe piloerection, slow or no response to stimuli, labored breathing, or rectal prolapse; or any three of: moderate hunching, moderate piloerection, some lethargy, some change in breathing rate, effort or pattern), mice were euthanized by isoflurane anesthesia followed by carbon dioxide inhalation.

Luminescence assay

Strains harbouring *lux* reporters were cultured in triplicate overnight in LB with kanamycin, then subcultured 1:100 into the same medium. After 3 h growth at 37ºC with aeration, 100 µl of each culture was transferred to a black/clear bottom 96-well plate and dithiothreitol was added where indicated. Luminescence and OD_{600} were measured every 5 min for 2 h using a Tecan Infinite 200 plate reader. Normalized luminescence was calculated by dividing raw luminescence by the OD_{600} of the same well.

Acknowledgements

This work was supported by grants from the Canadian Institutes of Health Research (MOP-136976 to B.B.F., MOP-342982 to T.L.R., and MOP-77688 to L.J.F.). S.L.V. was the recipient of a Killam Postdoctoral Research Fellowship, a Michael Smith Foundation for Health Research Postdoctoral Fellowship, and a CIHR Postdoctoral Fellowship. N.E.S was supported by a by National Health and Medical Research Council of Australia Overseas (Biomedical) Fellowship (APP1037373). B.B.F. is the University of British Columbia Peter Wall Distinguished Professor. We are grateful to Samantha Gruenheid (McGill University) for sharing strains DBS100 *ΔcpxRA*, *ΔcpxRA::cpxRA* and *ΔcpxA* . We thank Wanyin Deng for invaluable discussions and advice and Kristie Keeney for assistance with the animal experiments.

Author Contributions

S.L.V., R.S., R.L.G., T.L.R., and B.B.F. conceived the study and designed experiments; S.L.V., R.S., Y.P., R.L.G., N.E.S., and S.E.W. performed experiments; S.L.V., R.S., and N.E.S.

711 analyzed data; and S.L.V., R.S., N.E.S., L.J.F., T.L.R., and B.B.F. wrote the paper. All authors
712 reviewed the results and approved the final version of the manuscript.
713
714 **References**

715 Belin, P., and Boquet, P.L. (1994) The *Escherichia coli dsbA* gene is partly transcribed from the
716 promoter of a weakly expressed upstream gene. *Microbiology* **140**: 3337–3348.
717 Brown, N.F., Rogers, L.D., Sanderson, K.L., Gouw, J.W., Hartland, E.L., and Foster, J. (2014) A
718 horizontally acquired transcription factor coordinates *Salmonella* adaptations to host
719 microenvironments. *MBio* **5**: e01727-14.
720 Caballero-Flores, G.G., Croxen, M.A., Martínez-Santos, V.I., Finlay, B.B., and Puente, J.L.
721 (2015) Identification and regulation of a novel *Citrobacter rodentium* gut colonization fimbria
722 (Gcf). *J Bacteriol* **197**: 1478–1491.
723 Cheng, C., Wakefield, M.J., Yang, J., Tauschek, M., and Robins-Browne, R.M. (2012) Genome-
724 wide analysis of the Pho regulon in a *pstCA* mutant of *Citrobacter rodentium*. *PLoS One* **7**:
725 e50682.
726 Choi, K.H., Gaynor, J.B., White, K.G., Lopez, C., Bosio, C.M., Karkhoff-Schweizer, R.A.R.,
727 and Schweizer, H.P. (2005) A Tn7-based broad-range bacterial cloning and expression system.
728 *Nat Methods* **2**: 443–448.
729 Cleary, J., Lai, L.C., Shaw, R.K., Straatman-Iwanowska, A., Donneberg, M.S., Frankel, G., and
730 Knutton, S. (2004) Enteropathogenic *Escherichia coli* (EPEC) adhesion to intestinal epithelial
731 cells: Role of bundle-forming pili (BFP), EspA filaments and intimin. *Microbiology* **150**: 527–
732 538.
733 Collins, J.W., Keeney, K.M., Crepin, V.F., Rathinam, V.A.K., Fitzgerald, K.A., Finlay, B.B.,
734 and Frankel, G. (2014) *Citrobacter rodentium*: Infection, inflammation and the microbiota. *Nat*
735 *Rev Microbiol* **12**: 612–623.
736 Cox, J., and Mann, M. (2008) MaxQuant enables high peptide identification rates, individualized
737 p.p.b.-range mass accuracies and proteome-wide protein quantification. *Nat Biotechnol* **26**:
738 1367–1372.
739 Croxen, M.A., Law, R.J., Scholz, R., Keeney, K.M., Wlodarska, M., and Finlay, B.B. (2013)
740 Recent advances in understanding enteric pathogenic *Escherichia coli*. *Clin Microbiol Rev* **26**:
741 822–80.

Danese, P.N., and Silhavy, T.J. (1997) The σ^E and the Cpx signal transduction systems control the synthesis of periplasmic protein-folding systems in *Escherichia coli*. *Genes Dev* **11**: 1183–1193.

Danese, P.N., and Silhavy, T.J. (1998) CpxP, a stress-combative member of the Cpx regulon. *J Bacteriol* **180**: 831–839.

Danese, P.N., Snyder, W.B., Cosma, C.L., Davis, L.J., and Silhavy, J. (1995) The Cpx two-component signal transduction pathway of *Escherichia coli* regulates transcription of the gene specifying the stress-inducible periplasmic protease, DegP. *Genes Dev* 387–398.

Datsenko, K.A., and Wanner, B.L. (2000) One-step inactivation of chromosomal genes in *Escherichia coli* K-12 using PCR products. *Proc Natl Acad Sci U S A* **97**: 6640–6645.

De la Cruz, M.A., Morgan, J.K., Ares, M.A., Yáñez-Santos, J.A., Riordan, J.T., and Girón, J.A. (2016) The two-component system CpxRA negatively regulates the locus of enterocyte effacement of enterohemorrhagic *Escherichia coli* involving σ^{32} and Lon protease. *Front Cell Infect Microbiol* **6**.

De la Cruz, M.A., Pérez-Morales, D., Palacios, I.J., Fernández-Mora, M., Calva, E., and Bustamante, V.H. (2015) The two-component system CpxR/A represses the expression of *Salmonella* virulence genes by affecting the stability of the transcriptional regulator HilD. *Front Microbiol* **6**: 1–14.

Deng, W., Hoog, C.L. De, Yu, H.B., Li, Y., Croxen, M.A., Thomas, N.A., *et al.* (2010) A comprehensive proteomic analysis of the type III secretome of *Citrobacter rodentium*. *J Biol Chem* **285**: 6790–6800.

Deng, W., Puente, J.L., Gruenheid, S., Li, Y., Vallance, B.A., Vázquez, A., *et al.* (2004) Dissecting virulence: systematic and functional analyses of a pathogenicity island. *Proc Natl Acad Sci U S A* **101**: 3597–602.

Deng, W., Vallance, B.A., Li, Y., Puente, J.L., and Finlay, B.B. (2003) *Citrobacter rodentium* translocated intimin receptor (Tir) is an essential virulence factor needed for actin condensation, intestinal colonization and colonic hyperplasia in mice. *Mol Microbiol* **48**: 95–115.

Dorsey-Oresto, A., Lu, T., Mosel, M., Wang, X., Salz, T., Drlica, K., and Zhao, X. (2013) YihE kinase is a central regulator of programmed cell death in bacteria. *Cell Rep* **3**: 528–37.

Edwards, R.A., Keller, L.H., and Schifferli, D.M. (1998) Improved allelic exchange vectors and

their use to analyze 987P fimbria gene expression. *Gene* **207**: 149–157.
Ferrières, L., Hémery, G., Nham, T., Guérout, A.M., Mazel, D., Beloin, C., and Ghigo, J.M. (2010) Silent mischief: Bacteriophage Mu insertions contaminate products of *Escherichia coli* random mutagenesis performed using suicidal transposon delivery plasmids mobilized by broad-host-range RP4 conjugative machinery. *J Bacteriol* **192**: 6418–6427.
Girón, J.A., Ho, A.S.Y., and Schoolnik, G.K. (1991) An inducible bundle-forming pilus of enteropathogenic *Escherichia coli*. *Science (80-)* **254**: 710–713.
Guest, R.L., and Raivio, T.L. (2016) Role of the Gram-negative envelope stress response in the presence of antimicrobial agents. *Trends Microbiol* **24**: 377–390.
Hart, E., Yang, J., Tauschek, M., Kelly, M., Wakefield, M.J., Frankel, G., *et al.* (2008) RegA, an AraC-like protein, Is a global transcriptional regulator that controls virulence gene expression in *Citrobacter rodentium*. *Infect Immun* **76**: 5247–5256.
Hirano, Y., Hossain, M.M., Takeda, K., Tokuda, H., and Miki, K. (2007) Structural studies of the Cpx pathway activator NlpE on the outer membrane of *Escherichia coli*. *Structure* **15**: 963–976.
Ho, S.N., Hunt, H.D., Horton, R.M., Pullen, J.K., and Pease, L.R. (1989) Site-directed mutagenesis by overlap extension using the polymerase chain reaction. *Gene* **77**: 51–59.
Humphries, R.M., Griener, T.P., Vogt, S.L., Mulvey, G.L., Raivio, T., Donnenberg, M.S., *et al.* (2010) N-acetyllactosamine-induced retraction of bundle-forming pili regulates virulence-associated gene expression in enteropathogenic *Escherichia coli*. *Mol Microbiol* **76**: 1111–1126.
Jones, C.H., Danese, P.N., Pinkner, J.S., Silhavy, T.J., and Hultgren, S.J. (1997) The chaperone-assisted membrane release and folding pathway is sensed by two signal transduction systems. *EMBO J* **16**: 6394–6406.
Kamada, N., Kim, Y.-G., Sham, H.P., Vallance, B.A., Puente, J.L., Martens, E.C., and Núñez, G. (2012) Regulated virulence controls the ability of a pathogen to compete with the gut microbiota. *Science* **336**: 1325–1329.
Lasaro, M., Liu, Z., Bishar, R., Kelly, K., Chattopadhyay, S., Paul, S., *et al.* (2014) *Escherichia coli* isolate for studying colonization of the mouse intestine and its application to two-component signaling knockouts. *J Bacteriol* **196**: 1723–1732.
Love, M.I., Huber, W., and Anders, S. (2014) Moderated estimation of fold change and dispersion for RNA-seq data with DESeq2. *Genome Biol* **15**: 1–21.
MacRitchie, D.M., Acosta, N., and Raivio, T.L. (2012) DegP is involved in Cpx-mediated

posttranscriptional regulation of the type III secretion apparatus in enteropathogenic *Escherichia coli*. *Infect Immun* **80**: 1766–72.

MacRitchie, D.M., Ward, J.D., Nevesinjac, A.Z., and Raivio, T.L. (2008) Activation of the Cpx envelope stress response down-regulates expression of several locus of enterocyte effacement-encoded genes in enteropathogenic *Escherichia coli*. *Infect Immun* **76**: 1465–1475.

Magoc, T., Wood, D., and Salzberg, S.L. (2013) EDGE-pro: Estimated Degree of Gene Expression in prokaryotic genomes. *Evol Bioinforma* **2013**: 127–136.

Miki, T., Okada, N., Kim, Y., Abe, A., and Danbara, H. (2008) DsbA directs efficient expression of outer membrane secretin EscC of the enteropathogenic *Escherichia coli* type III secretion apparatus. *Microb Pathog* **44**: 151–158.

Mileykovskaya, E., and Dowhan, W. (1997) The Cpx two-component signal transduction pathway is activated in *Escherichia coli* mutant strains lacking phosphatidylethanolamine. **179**: 1029–1034.

Moon, H.W., Whipp, S.C., Argenzio, R.A., Levine, M.M., and Giannella, R.A. (1983) Attaching and effacing activities of rabbit and human enteropathogenic *Escherichia coli* in pig and rabbit intestines. *Infect Immun* **41**: 1340–1351.

Mundy, R., Girard, F., Fitzgerald, A.J., and Frankel, G. (2006) Comparison of colonization dynamics and pathology of mice infected with enteropathogenic *Escherichia coli*, enterohaemorrhagic *E. coli* and *Citrobacter rodentium*. *FEMS Microbiol Lett* **265**: 126–132.

Mundy, R., Pickard, D., Wilson, R.K., Simmons, C.P., Dougan, G., and Frankel, G. (2003) Identification of a novel type IV pilus gene cluster required for gastrointestinal colonization of *Citrobacter rodentium*. *Mol Microbiol* **48**: 795–809.

Nagamatsu, K., Hannan, T.J., Guest, R.L., Kostakioti, M., Hadjifrangiskou, M., Binkley, J., *et al.* (2015) Dysregulation of *Escherichia coli* α-hemolysin expression alters the course of acute and persistent urinary tract infection. *Proc Natl Acad Sci* **112**: E871–E880.

Nevesinjac, A.Z., and Raivio, T.L. (2005) The Cpx envelope stress response affects expression of the type IV bundle-forming pili of enteropathogenic *Escherichia coli*. *J Bacteriol* **187**: 672–686.

Pogliano, J., Lynch, A.S., Belin, D., Lin, E.C., and Beckwith, J. (1997) Regulation of *Escherichia coli* cell envelope proteins involved in protein folding and degradation by the Cpx two-component system. *Genes Dev* **11**: 1169–82.

835 Raivio, T.L. (2005) Envelope stress responses and Gram-negative bacterial pathogenesis. *Mol*
836 *Microbiol* **56**: 1119–1128.
837 Raivio, T.L. (2014) Everything old is new again: An update on current research on the Cpx
838 envelope stress response. *Biochim Biophys Acta - Mol Cell Res* **1843**: 1529–1541.
839 Raivio, T.L., Laird, M.W., Joly, J.C., and Silhavy, T.J. (2000) Tethering of CpxP to the inner
840 membrane prevents spheroplast induction of the Cpx envelope stress response. *Mol Microbiol*
841 **37**: 1186–1197.
842 Raivio, T.L., Leblanc, S.K.D., and Price, N.L. (2013) The *Escherichia coli* Cpx envelope stress
843 response regulates genes of diverse function that impact antibiotic resistance and membrane
844 integrity. *J Bacteriol* **195**: 2755–2767.
845 Raivio, T.L., Popkin, D.L., and Silhavy, T.J. (1999) The Cpx envelope stress response is
846 controlled by amplification and feedback inhibition. *J Bacteriol* **181**: 5263–5272.
847 Raivio, T.L., and Silhavy, T.J. (1997) Transduction of envelope stress in *Escherichia coli* by the
848 Cpx two-component system. *J Bacteriol* **179**: 7724–7733.
849 Rappsilber, J., Mann, M., and Ishihama, Y. (2007) Protocol for micro-purification, enrichment,
850 pre-fractionation and storage of peptides for proteomics using StageTips. *Nat Protoc* **2**: 1896–
851 1906.
852 Schroeder, B.O., Wu, Z., Nuding, S., Groscurth, S., Marcinowski, M., Beisner, J., *et al.* (2011)
853 Reduction of disulphide bonds unmasks potent antimicrobial activity of human β-defensin 1.
854 *Nature* **469**: 419–423.
855 Sherman, P., Soni, R., and Karmali, M. (1988) Attaching and effacing adherence of vero
856 cytotoxin-producing *Escherichia coli* to rabbit intestinal epithelium *in vivo*. *Infect Immun* **56**:
857 756–761.
858 Simmons, C.P., Goncalves, N.S., Ghaem-Maghami, M., Bajaj-Elliott, M., Clare, S., Neves, B., *et*
859 *al.* (2002) Impaired resistance and enhanced pathology during infection with a noninvasive,
860 attaching-effacing enteric bacterial pathogen, *Citrobacter rodentium*, in mice lacking IL-12 or
861 IFN-γ. *J Immunol* **168**: 1804–1812.
862 Snyder, W.B., Davis, L.J.B., Danese, P.N., Cosma, C.L., and Silhavy, T.J. (1995)
863 Overproduction of NlpE, a new outer membrane lipoprotein, suppresses the toxicity of
864 periplasmic LacZ by activation of the Cpx signal transduction pathway. *J Bacteriol* **177**: 4216–
865 4223.

Thomassin, J.-L., Giannakopoulou, N., Zhu, L., Gross, J., Salmon, K., Leclerc, J.-M., *et al.* (2015) The CpxRA two-component system is essential for *Citrobacter rodentium* virulence. *Infect Immun* **83**: 1919–28.

Thomassin, J.-L., Leclerc, J.-M., Giannakopoulou, N., Zhu, L., Salmon, K., Portt, A., *et al.* (2017) Systematic analysis of two-component systems in *Citrobacter rodentium* reveals positive and negative roles in virulence. *Infect Immun* **85**: e00654-16.

Tyanova, S., Temu, T., Carlson, A., Sinitcyn, P., Mann, M., and Cox, J. (2015) Visualization of LC-MS/MS proteomics data in MaxQuant. *Proteomics* **15**: 1453–1456.

Udeshi, N.D., Svinkina, T., Mertins, P., Kuhn, E., Mani, D.R., Qiao, J.W., and Carr, S.A. (2013) Refined Preparation and Use of Anti-diglycine Remnant (K-ε-GG) Antibody Enables Routine Quantification of 10,000s of Ubiquitination Sites in Single Proteomics Experiments. *Mol Cell Proteomics* **12**: 825–831.

Vallance, B.A., Deng, W., Jacobson, K., and Finlay, B.B. (2003) Host susceptibility to the attaching and effacing bacterial pathogen *Citrobacter rodentium*. *Infect Immun* **71**: 3443–3453.

Vizcaíno, J.A., Csordas, A., Del-Toro, N., Dianes, J.A., Griss, J., Lavidas, I., *et al.* (2016) 2016 update of the PRIDE database and its related tools. *Nucleic Acids Res* **44**: D447–D456.

Vogt, S.L., Nevesinjac, A.Z., Humphries, R.M., Donnenberg, M.S., Armstrong, G.D., and Raivio, T.L. (2010) The Cpx envelope stress response both facilitates and inhibits elaboration of the enteropathogenic *Escherichia coli* bundle-forming pilus. *Mol Microbiol* **76**: 1095–1110.

Vogt, S.L., and Raivio, T.L. (2012) Just scratching the surface: An expanding view of the Cpx envelope stress response. *FEMS Microbiol Lett* **326**: 2–11.

Willing, B.P., Vacharaksa, A., Croxen, M., Thanachayanont, T., and Finlay, B.B. (2011) Altering host resistance to infections through microbial transplantation. *PLoS One* **6**: 2–10.

Wlodarska, M., Willing, B., Keeney, K.M., Menendez, A., Bergstrom, K.S., Gill, N., *et al.* (2011) Antibiotic treatment alters the colonic mucus layer and predisposes the host to exacerbated *Citrobacter rodentium*-induced colitis. *Infect Immun* **79**: 1536–1545.

Wulf, P. De, Kwon, O., and Lin, E.C.C. (1999) The CpxRA signal transduction system of *Escherichia coli*: Growth-related autoactivation and control of unanticipated target operons. *J Bacteriol* **181**: 6772–6778.

Wulf, P. De, McGuire, A.M., Liu, X., and Lin, E.C.C. (2002) Genome-wide profiling of promoter recognition by the two-component response regulator CpxR-P in *Escherichia coli*. *J*

Biol Chem **277**: 26652–26661.

Zhang, H.Z., and Donnenberg, M.S. (1996) DsbA is required for stability of the type IV pilin of enteropathogenic *Escherichia coli*. *Mol Microbiol* **21**: 787–97.

Table 1. Transcripts and proteins differentially expressed in *C. rodentium ΔcpxRA* relative to DBS100 as determined by RNA-Seq and SILAC.

Gene symbol	Gene name	Product/description	Fold change WT/ *ΔcpxRA* (RNA-Seq)†	Fold change WT/ *ΔcpxRA* (SILAC)†
Envelope protein folding and turnover				
ROD_38372	*cpxP*	periplasmic adaptor for DegP-mediated proteolysis; negative regulator of the Cpx response	**66.45**	n.d.
ROD_10321	*yccA*	substrate or modulator of FtsH-mediated proteolysis	**52.19**	n.d.
ROD_18691	*htpX*	zinc-dependent endoprotease	**12.10**	10.77‡
ROD_28631	*ptrA*	protease III	**9.22**	0.93
ROD_13141	*spy*	ATP-independent periplasmic chaperone	**7.52**	**1.48**
ROD_23401	*eco*	ecotin; serine protease inhibitor	**7.33**	**4.55**
ROD_44461	*ppiA*	peptidyl-prolyl cis-trans isomerase	**2.68**	**2.52**
ROD_38991	*dsbA*	thiol:disulfide interchange protein	**2.06**	**1.33**
ROD_01651	*degP* (*htrA*)	periplasmic serine	**1.28**	**1.41**

		endoprotease		
Pili/fimbriae				
ROD_41251 – ROD_41291	*kfcCDEFG*	K99-type chaperone-usher fimbriae	**0.39 – 0.48**	0.46‡ (KfcC)
Type III secretion				
ROD_10831	*nleB1*	T3SS effector	**0.37**	**0.72**
ROD_16511	*nleG1*	T3SS effector	**0.39**	0.90‡
ROD_10841	*nleE*	T3SS effector	**0.40**	0.74
ROD_12111	*espK*	T3SS effector	**0.40**	n.d.
ROD_16491	*nleC*	T3SS effector	**0.43**	0.76‡
ROD_40971	*nleG8*	T3SS effector	**0.43**	n.d.
ROD_48891	*nleG7*	T3SS effector	**0.48**	n.d.
ROD_12071	*espX7*	T3SS effector	**0.49**	**0.74**
ROD_31791	*espM3*	T3SS effector	**0.50**	n.d.
ROD_03391	*espS*	T3SS effector	**0.71**	**0.41**
ROD_29741	*espB*	T3SS translocator protein	**1.23**	**0.46**
Other functions				
ROD_39001	*rdoA*	putative regulatory protein kinase	**2.78**	**1.62**
ROD_17451	*yciG*	putative protein	5.76	n.d.
ROD_17461	*yciF*	putative ruberythrin/ferritin-like metal-binding protein	**2.05**	**3.18**
ROD_17471	*yciE*	putative ruberythrin/ferritin-	**2.29**	**3.43**

		like metal-binding protein		
ROD_17481		Mn-containing catalase	0.69	**3.40**
ROD_21281	*pduE*	propanediol utilization dehydratase, small subunit	1.00	**0.28**
ROD_21251	*pduB*	propanediol utilization protein	1.07	**0.34**
ROD_21311	*pduJ*	propanediol utilization protein	1.26	**0.38**

†Bolded numbers indicate a significant difference in transcript or protein abundance between DBS100 and *ΔcpxRA*, FDR < 0.05.

‡Proteins for which only one peptide was detected by SILAC; see Materials and Methods

Figure Legends

Figure 1. Comparison of CpxAR's effect on the *C. rodentium* transcriptome and proteome. Venn diagrams show the numbers of transcripts or proteins differentially expressed at a cutoff of twofold in DBS100 and *ΔcpxRA* with a statistical cutoff of FDR < 0.05, as determined by RNA-Seq and SILAC, respectively. A) Transcripts/proteins positively regulated by CpxAR (more abundant in wild-type than in *ΔcpxRA*). B) Transcripts/proteins negatively regulated by CpxAR (more abundant in *ΔcpxRA* than in wild-type).

Figure 2. Validation of RNA-Seq and SILAC results. Selected transcripts and proteins identified as differentially expressed by RNA-Seq and/or SILAC were validated by RT-qPCR (A-C, E) or Western blotting (D), respectively. cDNA templates for RT-qPCR were prepared from strains grown in DMEM in biological triplicate cultures. Western blots were performed using whole-cell lysates from strains grown in DMEM. Significant differences in transcript

abundance in DBS100 and *ΔcpxRA* were assessed using multiple *t*-tests with the Holm-Sidak correction for multiple comparisons: *, $P<0.05$; **, $P<0.01$; ***, $P<0.001$.

Figure 3. *C. rodentium ΔdegP* and *ΔdsbA* mutants have aberrant secreted protein profiles. Proteins were precipitated from supernatants of strains grown in DMEM for 6 h, separated by 15% SDS-PAGE, and stained with Coomassie Brilliant Blue or detected by Western blot using α-EspB monoclonal antibodies. 2 µg of purified BSA was added to each collected supernatant to aid in protein precipitation.

Figure 4. *C. rodentium ΔdegP* and *ΔdsbA* are attenuated in the C3H/HeJ mouse model of infection. A) Survival of mice infected with wild-type and mutant strains of *C. rodentium*. Mice were monitored daily and euthanized upon reaching the humane endpoint described in Materials and Methods. * denotes $P<0.05$, Mantel-Cox test with Bonferroni's correction for multiple comparisons. B) Fecal shedding of *C. rodentium* throughout the course of infection. The connecting lines denote the mean and error bars denote standard deviation. LOD, limit of detection. Both panels show the combined results of six separate experiments, with a total of N=30 mice per strain for DBS100 and *ΔcpxRA*, N=20 mice per strain for *ΔdegP* and *ΔdsbA*, and N=5 mice per strain for *ΔcpxP*, *Δeco*, *ΔppiA*, *Δspy*, *ΔyccA*, and ΔROD_17451-81.

Figure 5. Defining the promoter region required for CpxR regulation of *degP*. A) Alignment of the *degP* promoter sequences from *E. coli* MG1655 (Eco) and *C. rodentium* ICC168 (Crod). The CpxR binding region identified by DNase footprinting in *E. coli* (Pogliano *et al.*, 1997) is identified with a red arrow, and two inverted CpxR binding motifs are identified with red boxes. The 25 bp region deleted in the *C. rodentium* promoter to give rise to $P_{degP\Delta CpxR}$ is shown with a blue box. Coordinates are relative to the translational start site. B) Activity of P_{degP}-*lux* and $P_{degP\Delta CpxR}$-*lux* reporters in wild-type and *ΔcpxRA* strains of *C. rodentium*. Data represent the mean and standard deviation of three biological replicate cultures. C) Transcript abundance of *degP* in wild-type and *ΔcpxRA* strains of *C. rodentium*, with chromosomal wild-type or $P_{degP\Delta CpxR}$ promoters, as measured by RT-qPCR. * denotes $P<0.05$ and **** denotes $P<0.0001$, one-way ANOVA with Sidak's multiple comparison test; n.s., no significant difference.

Figure 6. Defining the promoter region required for CpxR regulation of *dsbA*. A) Activity of P_{rdoA}-*lux* and P_{dsbA}-*lux* reporters in wild-type and *ΔcpxRA* strains of *C. rodentium*. B) Alignment of the *rdoA* promoter sequences from *E. coli* MG1655 (Eco) and *C. rodentium* ICC168 (Crod). The CpxR binding region identified by DNase footprinting in *E. coli* (Pogliano *et al.*, 1997) is identified with a red arrow, and two CpxR binding motifs are identified with red boxes. The three substitution mutations introduced into the *C. rodentium* promoter to give rise to $P_{rdoA\text{mut}}$ are shown in blue. The coding sequence of the gene upstream of *rdoA* (ROD_39011) is underlined. Coordinates are relative to the translational start site. C) Activity of P_{rdoA}-*lux* and $P_{rdoA\text{mut}}$-*lux* reporters in wild-type and *ΔcpxRA* strains of *C. rodentium*. D) and E) Transcript abundance of *rdoA* (D) and *dsbA* (E) in wild-type and *ΔcpxRA* strains of *C. rodentium*, with chromosomal wild-type or $P_{rdoA\text{mut}}$ promoters, as measured by RT-qPCR. Data from luminescence assays represent the mean and standard deviation of three biological replicate cultures. * denotes $P<0.05$, ** denotes $P<0.01$, *** denotes $P<0.001$ and **** denotes $P<0.0001$, one-way ANOVA with Sidak's multiple comparison test; n.s., no significant difference.

Figure 7. Cpx regulation of *degP* and *dsbA* is not essential for infection of C3H/HeJ mice. A) Survival of mice infected with wild-type and mutant strains of *C. rodentium*. Mice were monitored daily and euthanized upon reaching the humane endpoint described in Materials and Methods. * denotes $P<0.05$, Mantel-Cox test with Bonferroni's correction for multiple comparisons. B) Fecal shedding of *C. rodentium* throughout the course of infection. The connecting lines denote the mean and error bars denote standard deviation. LOD, limit of detection. Both panels show the combined results of six separate experiments, with a total of N=30 mice per strain for DBS100 and *ΔcpxRA*, N=20 mice per strain for *ΔdegP* and *ΔdsbA*, N=10 mice per strain for $P_{degP\Delta\text{CpxR}}$ $P_{rdoA\text{mut}}$, and N=5 mice per strain for $P_{degP\Delta\text{CpxR}}$ and $P_{rdoA\text{mut}}$.

Figure 8. Disruption of disulfide bonding activates the Cpx pathway in *C. rodentium*. A) Activity of P_{cpxP}-*lux* reporter in wild-type and mutant strains of *C. rodentium*. B) Activity of P_{cpxP}-*lux* reporter in wild-type *C. rodentium* in the presence of DTT. Data from luminescence

assays represent the mean and standard deviation of three biological replicate cultures. **** denotes $P<0.0001$, one-way ANOVA with Dunnett's multiple comparison test.

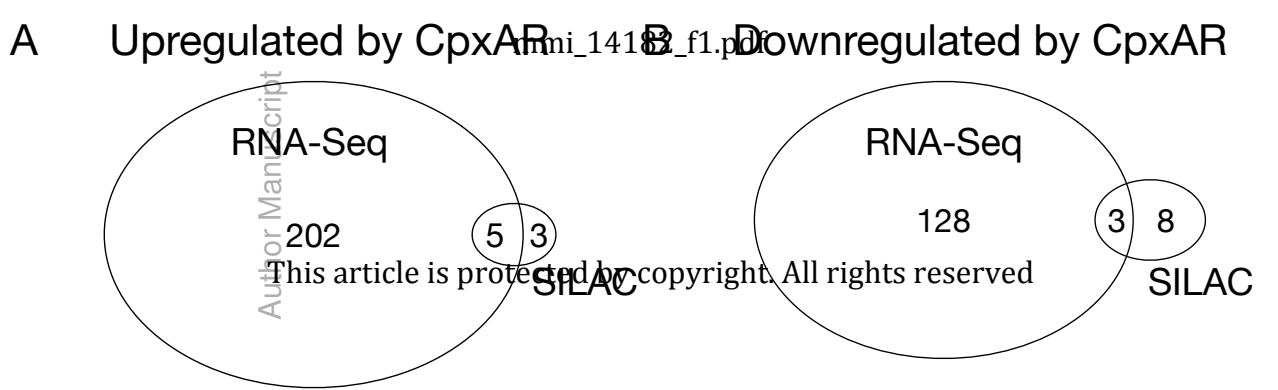

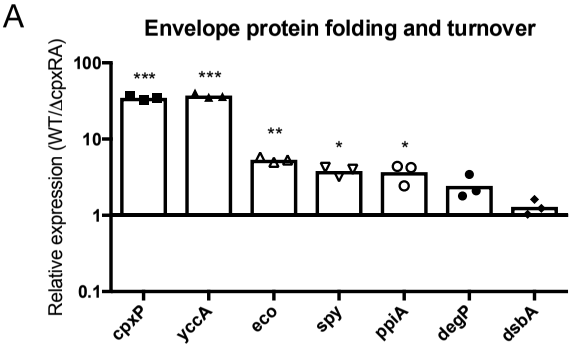

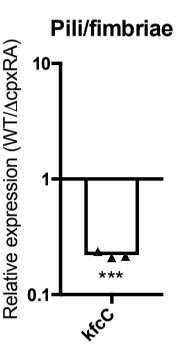

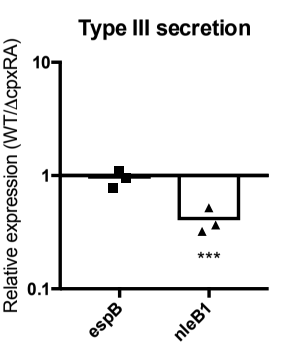

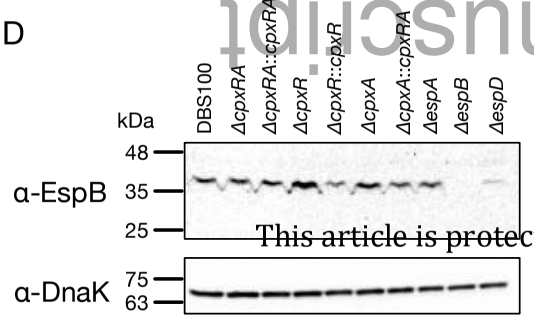

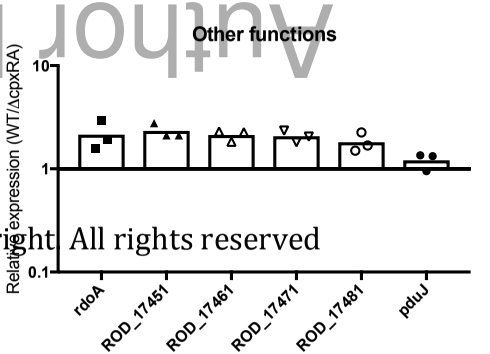

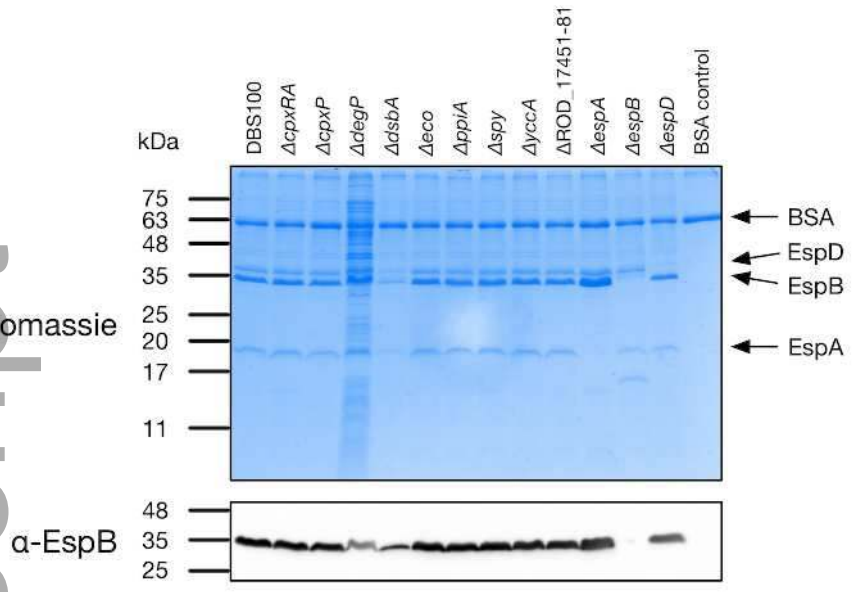

mmi_14182_f3.tiff

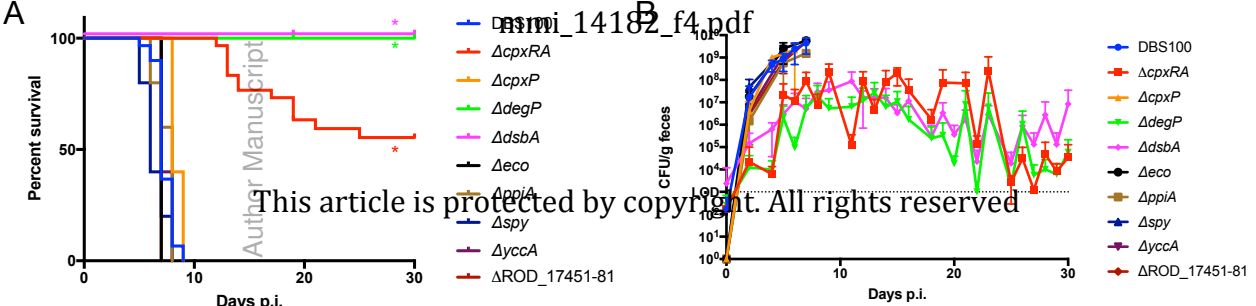

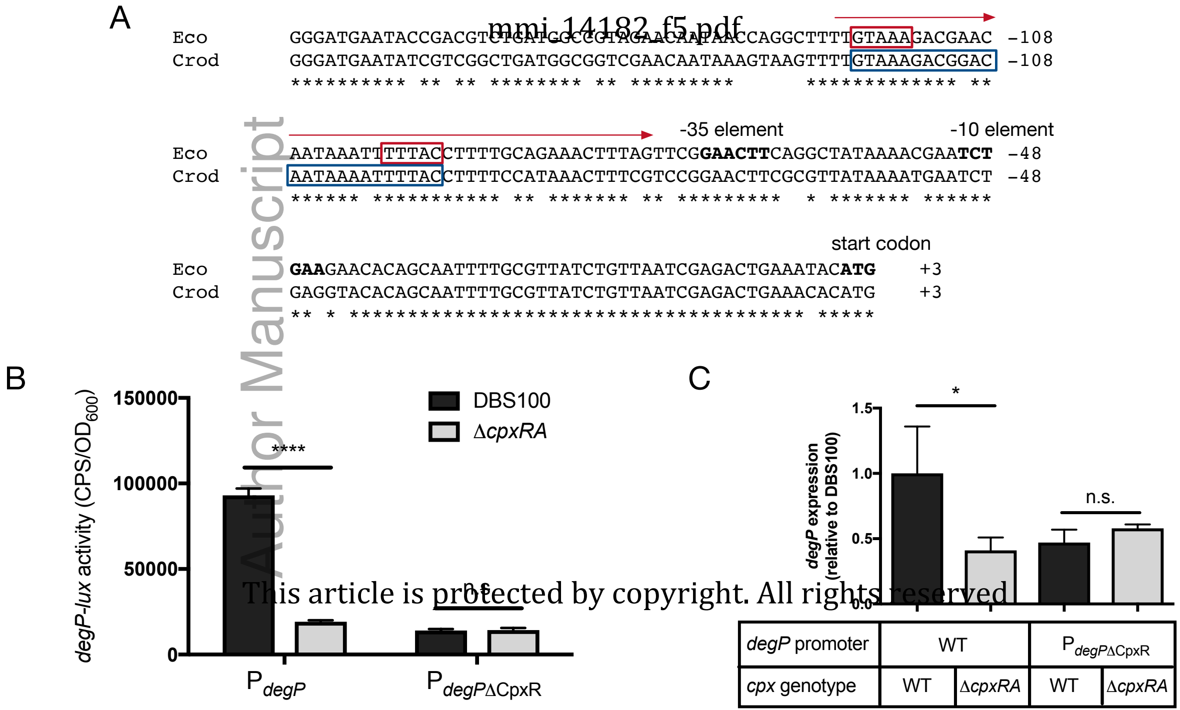

mmi_14182_f6_ndf

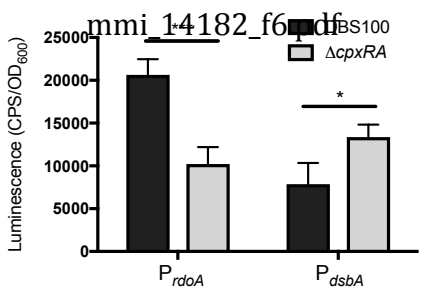

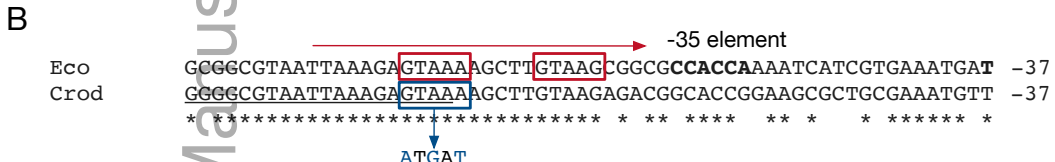

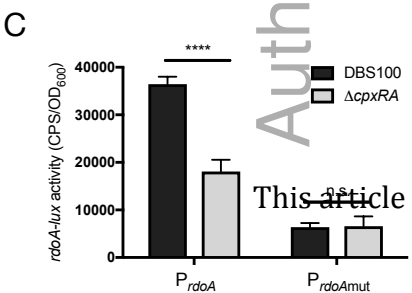

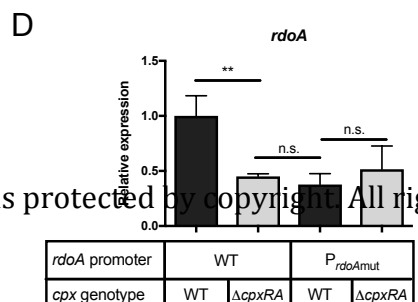

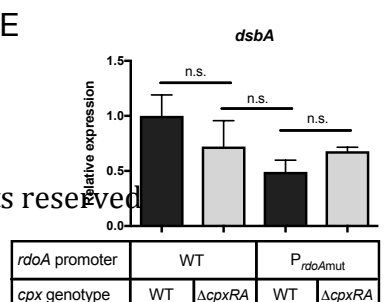

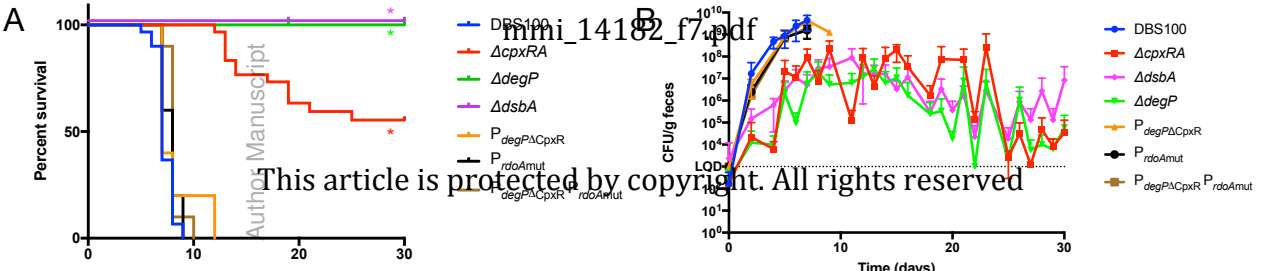

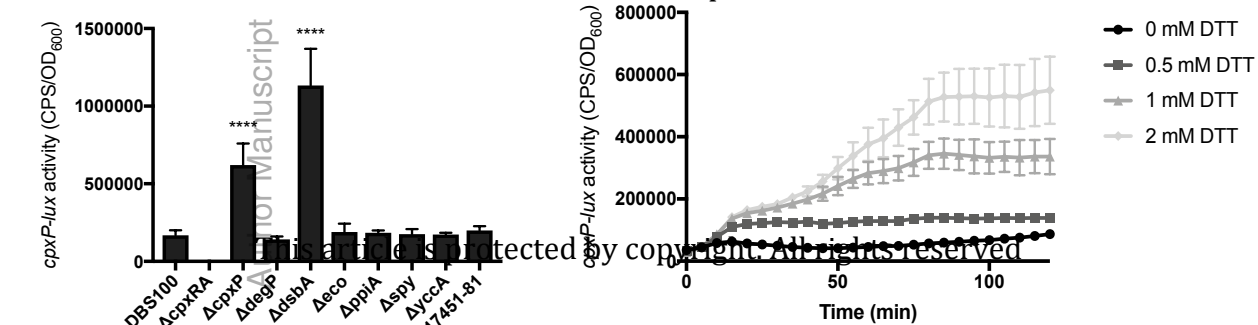

Author/s:
Vogt, SL;Scholz, R;Peng, Y;Guest, RL;Scott, NE;Woodward, SE;Foster, LJ;Raivio, TL;Finlay, BB

Title:
Characterization of the Citrobacter rodentium Cpx regulon and its role in host infection

Date:
2019-03-01

Citation:
Vogt, S. L., Scholz, R., Peng, Y., Guest, R. L., Scott, N. E., Woodward, S. E., Foster, L. J., Raivio, T. L. & Finlay, B. B. (2019). Characterization of the Citrobacter rodentium Cpx regulon and its role in host infection. MOLECULAR MICROBIOLOGY, 111 (3), pp.700-716. https://doi.org/10.1111/mmi.14182.